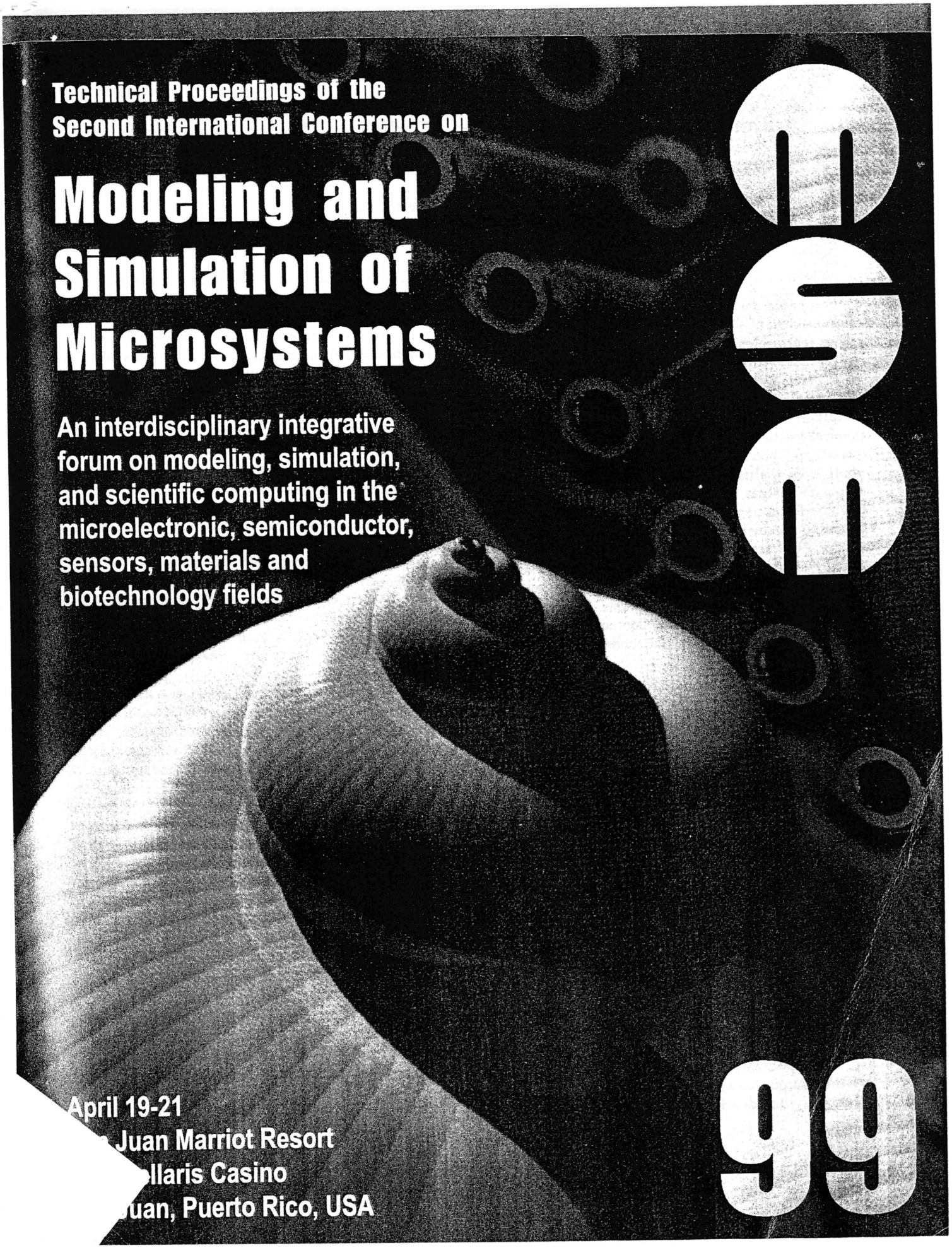
Technical Proceedings of the
Second International Conference on
Modeling and Simulation of Microsystems
An interdisciplinary integrative forum on modeling, simulation, and scientific computing in the microelectronic, semiconductor, sensors, materials and biotechnology fields
MSM
99
April 19-21
Juan Marriot Resort
llaris Casino
uan, Puerto Rico, USA

A Technique for Extraction of Macro-Models in System Level Simulation of Inertial Electro-Mechanical Micro-Systems

M. H. Zaman, S. F. Bart, V. L. Rabinovich, C. K. Ghaddar, I. Tchertkov, and J. R. Gilbert

Microcosm Technologies, Inc.
215 First Street, Suite 219, Cambridge, MA 02142, USA, zaman@memcad.com

ABSTRACT

This paper describes a systematic method for modeling the class of electro-mechanical micro-systems that can be represented as multi-component, lumped, mass-spring-dashpot structures. Examples include accelerometers, gyros, and other structures that have rigid masses and compliant springs. In this lumped modeling assumption, the lumped spring effect originates from mechanical reaction forces and moments of the suspensions (or tethers) holding the proof-mass. Damping forces result from multiple energy loss mechanisms, but are dominated by gas viscosity. In addition, there are electrostatic forces and torques exerted on the dielectrically separated conductors in the system when voltages are applied. The accuracy of the developed method is verified by comparison of two plate-tether MEMS structures to results obtained from the developed models with those from full 3-D physics simulations. Good accuracy is demonstrated in both spatial-domain and frequency-domain dynamic behavior of the models.

Keywords: Micro-system, MEMS, macro-model, simulation.

INTRODUCTION

The ability of MEMS devices to be integrated with signal conditioning circuitry and batch fabricated offers an important advantage over their macroscopic counterparts. To ensure proper functioning of such an integrated system, one must perform system-level simulation. Such system-level modeling is extremely useful in determining operation characteristics and verifying performance before the device is actually manufactured. This can reduce the need for prototype fabrication and test iterations and significantly reduce time-to-market. Thus, macro-model construction is a key part of a design methodology.

Performing full 3-D physical simulation within each time step of a typical system simulator (such as SABER, MATLAB, or SPICE) is prohibitively time-consuming and numerically impractical. Hence, in order to simulate the appropriate system level dynamic behavior efficiently, a reduced-ordered model or "macro-model" of the MEMS subsystem must be obtained and employed in the system-level simulator.

As micro-systems become more complex and the need for models with large numbers of coupled degrees-of-freedom (DOFs) increases, the use of automated tools for generating macro-models becomes increasingly important. Although macro-modeling techniques have been reported by some researchers ([2], [3]), currently there is no systematic method for generating macro-models for MEMS devices in an automatic way.

This paper describes a semi-automatic and complete modeling procedure that automates the generation of component-level macro-models of MEMS devices. The user assembles the system-level model by connecting individual component-level macro-models together. For simplicity, the developed method assumes that while the tethers provide mechanical compliance, they are electrostatically inert and massless. It also assumes that the proof mass is electrostatically driven and moves as a rigid body. Devices that do not move as a rigid body, such as membrane devices cannot be accurately modeled in this technique.

The procedure begins by dividing the whole device into sub-components such as mechanical springs, electrostatic elements, dashpots, and proof-masses. These subcomponents are separately meshed and simulated in finite element method (FEM) and boundary element method (BEM) solvers over the desired ranges of operation. These full 3-D physics simulations are done in MEMCAD [8] using hybrid finite element and accelerated boundary element physics. The results of these simulations are fitted to multi-variable polynomials as functions of the desired DOFs. The macro-models for each subcomponent are then automatically generated in the behavioral modeling language of a system level simulator (SABER, SPICE, etc.). Finally, the component-level macro-models are assembled into a system-level design to model the behavior of the whole system.

THEORY

The modeling approach assumes coupling between three translational degrees of freedom (DOFs) and three rotational DOFs. While the translational DOFs are aligned with the axes of a general three-dimensional co-

ordinate system, a rather complex notation is used to denote the rotational degrees. According to Euler, any rigid body rotation can be described as one effective rotation around an arbitrarily oriented rotational axis.

The effective rotation θ is defined by its three components θ_x, θ_y, and θ_z as follows:

$$|\theta| = \sqrt{\theta_x^2 + \theta_y^2 + \theta_z^2}$$

The unit rotation vector is defined as

$$a\hat{i} + b\hat{j} + c\hat{k} = \frac{1}{|\theta|}(\theta_x\hat{i} + \theta_y\hat{j} + \theta_z\hat{k})$$

Hence, the position vector is comprised of three translations and three rotations:

$$\boldsymbol{x} = [x\ y\ z\ \theta_x\ \theta_y\ \theta_z]^T$$

The complete system model is expressed as a set of equations for each of these degrees of freedom. The complete system assumes equilibrium in total system energy. Equilibrium in the DOFs is achieved by balancing the total force and torque acting on the system. For a typical mass-spring-dashpot structure, the force-balance takes the following form:

$$f_{ext} = f_s + f_e + f_d + f_m \tag{1}$$

where f_{ext} is the force applied by external acceleration or other force sources (if any), f_s is the mechanical spring reaction force, f_e is the electrostatic force, f_d is the damping force, and f_m is the inertial force experienced by the proof mass. The torque-balance equation takes a form similar to Eq. 1. In the general case, Eq. 1 is a vector equation in six degrees of freedom, $\boldsymbol{x}$, and all fs are matrices. Each matrix element of f can be expanded in a Taylor series where we can choose the number of terms we care to retain. For example, a constant term in f_s represents a simple linear spring constant in a system where the degrees of freedom are uncoupled, $f_s = k_s\boldsymbol{x}$. In a six DOF system, k_s can be represented by a polynomial hyper-surface coupled in six degrees of freedom. In the work described here we keep terms up to fourth order. The coefficients of these polynomial expressions are found from full 6-D simulations of different physical effects (described below).

Component Level Equations of Motion

The equations of motion for the total structure are found by combining the mathematical model for each individual component. Following is a brief description of the system equations of a few representative MEMS components:

1. *Proof Mass:* A proof mass in a MEMS system is described by its mass, constant moments of inertia in its body-centered fixed coordinate system, and its center of mass. In a multi-DOF system, the coupling and interaction between the translational and rotational DOFs results in complex equations of motion for the proof-mass dynamics. A well-known part of this complex cross-coupling is the Coriolis effect. In order to be able to accurately predict the coupling between different DOFs and the dynamic motion of the proof-mass, one must retain the rotational coupling terms.

   Force Equations: The forces along the linear DOFs are given by [1]:

   $$F = m(\dot{v} + \omega \times v) \tag{2}$$

   where F is the force vector and m and v are respectively mass and linear velocities.

   Hence, the force components are given by

   $$m\begin{bmatrix} \ddot{x} \\ \ddot{y} \\ \ddot{z} \end{bmatrix} + m\begin{bmatrix} 0 & -\omega_z & \omega_y \\ \omega_z & 0 & -\omega_x \\ -\omega_y & \omega_x & 0 \end{bmatrix}\begin{bmatrix} \dot{x} \\ \dot{y} \\ \dot{z} \end{bmatrix} \tag{3}$$

   Moment Equations: The moments around the center-of-mass coordinate axes are given by [1]:

   $$M = \dot{H} + \omega \times H \tag{4}$$

   where M is the moment vector and m, v, H, and ω are respectively mass, velocity vector, angular momentum vector, and angular velocity vector. The angular momentum H is computed from the moment of inertia matrix and the angular velocity vector:

   $$\begin{bmatrix} H_x \\ H_y \\ H_z \end{bmatrix} = \begin{bmatrix} I_{xx} & -I_{xy} & -I_{xz} \\ -I_{yx} & I_{yy} & -I_{yz} \\ -I_{zx} & -I_{zy} & I_{zz} \end{bmatrix}\begin{bmatrix} \omega_x \\ \omega_y \\ \omega_z \end{bmatrix} \tag{5}$$

   To avoid computation of varying moments of inertia of the proof-mass in the global coordinate system, these equations are computed in a frame of reference firmly attached at the body center of the proof-mass, thus making it subject to the rotations and translations that the mass experiences. The forces and moments so computed are then transformed to the global coordinate system in order to perform system-level simulation.

   The moment equations in the global coordinate system are found by

   $$M_{XYZ} = T\, M_{xyz} \tag{6}$$

   where T is the transformation matrix between the global (XYZ) and local (xyz) coordinate systems.

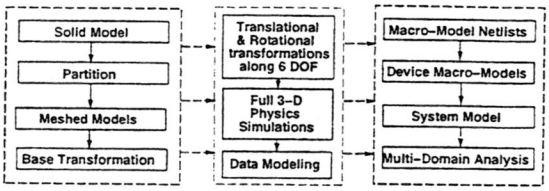

Figure 1: Sequence of Operations

2. Tether: The forces and moments exerted by a mechanical tether are represented by:

$$f_s = k_s x$$

where k_s is a combination of different order matrices with coupling coefficients between different DOFs.

3. Electrostatic Elements: Electrostatic forces are found by computing the spatial derivative of electrostatic energy:

$$f_e = \frac{1}{2} V^T \frac{d[C_{ij}]}{dx} V \qquad (7)$$

Equation 7 yields the electrostatic force as a function of one degree of freedom (x). Generalizing this to n degrees of freedom, the derivative becomes the spatial derivative of the n-dimensional capacitance surface.

4. Damper: The forces and moments exerted by a damper are computed by the following equation:

$$f_d = k_d \dot{x}$$

where k_d is the damping coefficient matrix and $\dot{x}$ is the spatial first-derivative of the DOF vector x.

Reusable Components

Most practical inertial MEMS devices contain multiple tethers and one or more electrostatic structures (e.g., combs), which are connected to the proof mass at multiple positions and orientations. Since these components are typically identical, one would like to perform detailed 3-D analysis only once and use the resulting model at multiple locations in the system model.

In the developed modeling technique, the mechanical springs and electrostatic force elements are simulated as independent entities in their local coordinate system. This allows them to be used in any device model with the help of converters that transform the degrees of freedom (translational and rotational), forces, and moments between these two systems. Another set of transformations are needed to transform the forces and torques applied by the spring at the location where it is connected to the

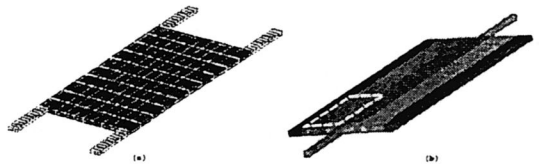

Figure 2: (a) Finite element mesh of example plate-tether structure, (b) Dominant mode-shape in Rotational-Y degree of freedom for example torsional mirror. (Dotted line shows approximate position and size of electrode underneath the plate).

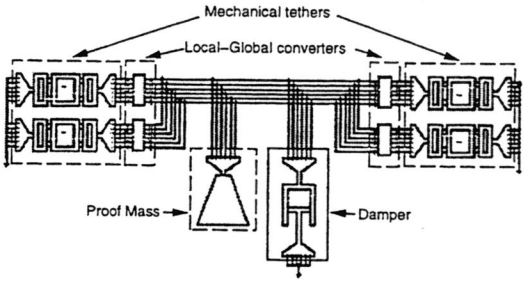

Figure 3: Schematic of the plate-tether structure model build from lumped elements (Through Variables: force, torque, current; Across Variables: position, angle, voltage)

center of mass of the proof mass. This allows the proof mass to be treated as a rigid body with its mass concentrated at its center of mass. These transformations include various types of Euler's and rotational transformations (and their inverse transformations) between coordinate systems.

IMPLEMENTATION

The modeling technique has been implemented in a tool named AutoMM (Auto Macro Modeler). The basic steps involve exploring the device operation space, modeling the data through multi-degree polynomial curve-fitting, and using the polynomial coefficients and other simulation data in dynamic equations. AutoMM consists of several sub-modules that are used to simulate the

Degrees of Freedom	AutoMM	Full 3-D	% Error
Translational X	811.91K	825.23K	-1.61
Translational Y	4421.7K	4342.8K	+1.82
Translational Z	433.39K	431.06K	+0.54
Rotational X	920.52K	939.29K	-1.99
Rotational Y	716.11K	710.70K	+0.76
Rotational Z	3439.8K	3428.8K	+0.32

Table 1: Comparison of modal frequencies obtained from AutoMM model and full 3-D physics simulation for plate-tether structure in Figure 2(a).

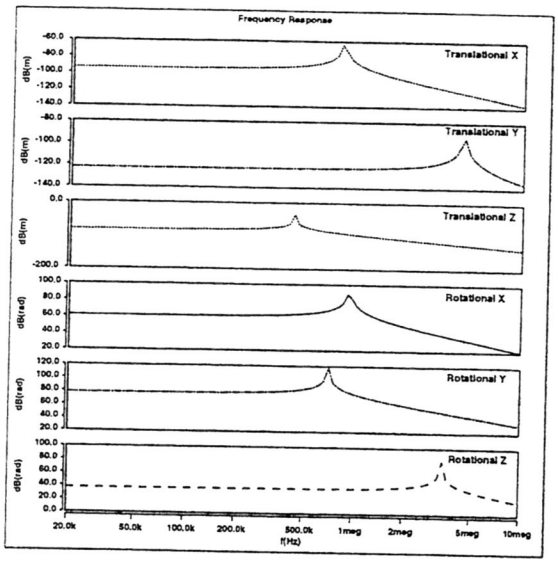

Figure 4: Frequency response in six degrees of freedom for the plate-tether structure in Figure 2(a).

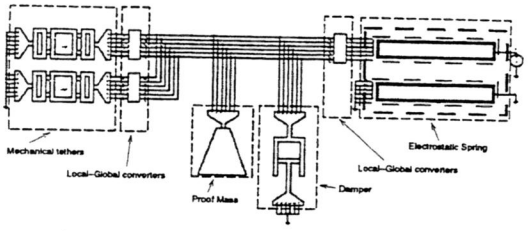

Figure 5: Schematic of torsional mirror model.

electrostatic, mechanical and inertial behavior of MEMS components in their operation space as a function of the DOFs.

AutoMM is built around the basic functionalities of the MEMCAD software tool suite [8]. It directly uses the MEMCAD device creation and visualization methods and applies wrappers around the solver modules. AutoMM is constructed as a collection of functional submodules. This allows the flexible addition of components with different physical behaviors. It also allows the calculation of the behavioral data to be done in parallel which reduces the over-all time of macro-model generation.

Sequence of Operations

Figure 1 shows the sequence of operations that are carried out by the AutoMM module to generate macro-models. The procedure starts by creating the device solid model using the 'MemBuilder' module of MEMCAD [8] from the device process information and the device layout. Then a finite-element mesh is created on the solid model. This meshed solid model is input

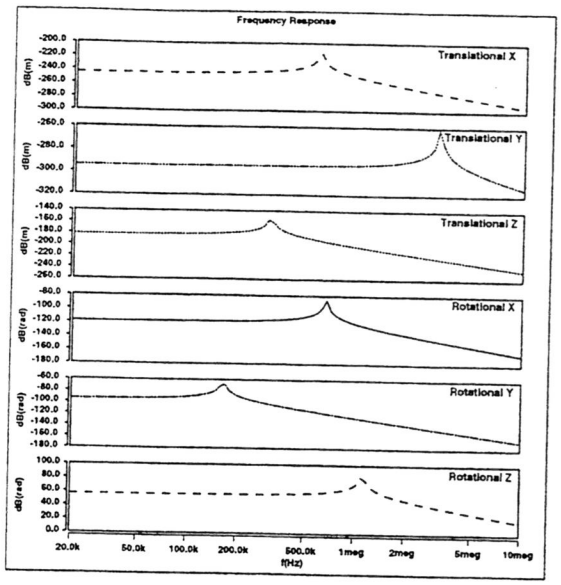

Figure 6: Frequency response in six degrees of freedom for torsional mirror in Figure 2(b).

to the AutoMM module which first carries out a global base transformation on the meshed structure according to the specifications provided by the designer. Examples of such transformations include changing separations of structures, angular orientations, lengths, thicknesses, density, Poisson ratio, stress, and other geometrical and material properties of different subsets of device components. Note that this step can account for the effects of manufacturing variations in the final device macro-model.

The transformed models are then passed to the submodules that perform electrostatic, mechanical, and inertial simulations using multi-DOF boundary conditions. The simulation data are then fit to multi-degree polynomial equations (up to fourth order), which are functions of the degrees of freedom over which the device has been simulated. These polynomial fit coefficients are finally used in system equations to create the device macro-model. Although most of these steps are automated, user interactions and interventions have been allowed in a few cases to include the capability of monitoring the simulation process and specification of user-defined macro-model parameters.

VERIFICATION

In order to verify the accuracy of this modeling technique, we have examined several MEMS structures. Here we present results for two of them. The first one is a simple horizontal plate structure with four parallel tethers at the four corners. Figure 2(a) shows the mass-spring meshed structure. Figure 3 shows the equivalent system model implemented in the SABER simulation tool. The

Degrees of Freedom	AutoMM	Full 3-D	% Error
Translational X	593.19K	583.53K	+1.66
Translational Y	3034.0K	3070.8K	-1.20
Translational Z	297.38K	304.82K	-2.44
Rotational X	672.54K	664.19K	+1.26
Rotational Y	169.02K	165.36K	+2.21
Rotational Z	1111.3K	1138.3K	-2.37

Table 2: Comparison of modal frequencies obtained from AutoMM model and full 3-D physics simulation for torsional mirror in Figure 2(b).

DOF	*25 Volts*			*150 Volts*		
	F3D	AM	%E	F3D	AM	%E
Tz (nm)	-1.60	-1.56	2.5	-65	-60	7.7
Rx (μ rad)	2.526	2.46	1	102.5	89.6	12.6
Ry (μ rad)	40.95	39.5	3.5	1700	1550	8.8

Table 3: Comparison of displacements and rotations in the dominant DOFs between full 3-D simulation and AutoMM results for two voltages (pull-in occurs at 219 volts). F3D, AM, and %E indicate full 3-D physics simulation results, AutoMM results, and percentage errors, respectively.

results of the lumped modeling technique are compared to the resonant frequency results of full 3-D physics simulation. Figure 4 shows the frequency response from the model for all DOFs. Table 1 compares the modal frequencies found from the model and full 3-D physics simulation, which show good agreement.

A torsional mirror with a ground electrode was also investigated. The ground electrode is under one of the corner of the plate and the plate is suspended by two tethers. A voltage applied between the plate and the electrode tilts the mirror assymetrically towards the fixed electrode. Figure 2(b) shows a dominant mode-shape of the structure found from full 3-D physics simulation. Figure 5 shows the equivalent system model. Figure 6 shows the frequency response from the model and Table 2 compares the corresponding modal frequencies with those obtained from full 3-D physics simulation. Table 3 compares the changes in the dominant DOFs with applied voltage. The displacements and rotations show reasonable agreement to those found from the MEMCAD coupled, full 3-D electromechanical solver. The observed results also show that the error increases as the applied voltage gets close to the pull-in voltage.

CONCLUSION

We have demonstrated a modeling procedure that automates the generation of macro-models of MEMS devices and shows good agreement to full 3-D physics simulation. The implemented modeling technique is currently limited to the class of devices where the actuating and restoring forces are limited to electrostatic, mechanical (tensile and torsional), damping, and inertial types. Future developments will consider electrostatically active mechanical tethers with nonzero mass and macromodels for other physical forces, such as fluidic pressure, thermal stress, piezo-electric potential, etc.

REFERENCES

[1] I. H. Shames, *Engineering Mechanics. Statics and Dynamics.* New Jersey: Prentice Hall, 1997.

[2] R. Neul, U. Becker, G. Lorenz, P. Schwarz, J. Hasse, and S. Wünsche, "A Modeling Approach to Include Mechanical Microsystem Componets into the System Simulation", in *DATE'98 - Design, Automation and Test in Europe*, vol. 1, pp.510-517, Feb, 1998.

[3] G. K. Fedder and R. T. Howe, "Multimode Digital Control of a Suspended Polysilicon Microstructure", *Journal of Microelectromechanical Systems*, pp. 283-297, May, 1996.

[4] N. R. Swart, S. F. Bart, M. H. Zaman, M. Mariappan, J. R. Gilbert, and D. Murphy, "AutoMM: Automatic Generation of Dynamic Macromodels for MEMS Devices," *Proc. 11th IEEE Intl. Workshop on Micro Electromechanical Systems (MEMS'98)*, pp. 178-183, Heidelberg, Germany, January 25-29, 1998.

[5] S. F. Bart, *CAD for Integrated Surface-Micromachined Sensors: Present and Future*, in the Proceedings of the Fifth ACM/SIGDA Physical Design Workshop, Reston, VA, April 15-17, pp. 72-75, 1996.

[6] G. Lorenz and R. Neul, "Network-Type Modeling of Micromachined Sensor Systems", *Proceedings of 1998 International Conference on Modeling and Simulation of Microsystems, Semiconductors, Sensors and Actuators* (MSM'98), pp. 233-238, Santa Clara, California, USA, April 6-8, 1998.

[7] S. D. Senturia, *CAD for Microelectromechanical Systems*, International Conference on Solid-State Sensors and Actuators, Transducers'95, Stockholm, June 26-29, 1995.

[8] *MEMCAD 4 Manual*, Microcosm Technologies, Inc., 5511 Capital Center Dr., Raleigh, NC, 1999.

[9] S. F. Bart, N. R. Swart, M. Mariappan, M. H. Zaman, and J. R. Gilbert, "An Enviroment for MEMS Design and Verification," *Proceedings of 1998 International Conference on Modeling and Simulation of Microsystems, Semiconductors, Sensors and Actuators* (MSM'98), pp. 386-391, Santa Clara, California, USA, April 6-8, 1998.